
Protein Fluorescence Measurements within Electrospray Droplets

Sandra E. Rodriguez-Cruz, Joseph T. Khoury and Joel H. Parks

The Rowland Institute for Science, 100 Edwin H. Land Boulevard, Cambridge, Massachusetts, USA

The conformation of cytochrome *c* molecules within electrospray droplets is investigated by monitoring the laser induced fluorescence of its single tryptophan residue (Trp-59). By increasing the alcohol concentration of the electrosprayed solutions, protein denaturation is induced, giving rise to significant changes in the intensity of the detected fluorescence. Comparison with analogous denaturation experiments in solution provides information about the relative protein conformations and differences between the bulk-solution and droplet environments. Both electrospray-plume and bulk-solution fluorescence measurements using low methanol concentration solutions indicate the presence of folded protein structures. At high methanol content, fluorescence measurements are consistent with the presence of partly denatured or unfolded conformations. At intermediate methanol content, differences are observed between the extent of denaturation in solution and that within the droplets, suggesting electrosprayed proteins have more compact structures than those detected in bulk measurements using solutions of similar composition. This infers that some fraction of the proteins within the droplets have refolded relative to their bulk-solution conformation. Protein denaturation experiments using the low vapor pressure solvent 1-propanol indicate that differences between the droplet and solution measurements are not due to solvent evaporation effects. It is suggested that different droplet conformations are more likely the result of protein diffusion to the droplet surface and effects of the droplet/air interface. To our knowledge, these are the first reported measurements of protein fluorescence within electrospray droplets (J Am Soc Mass Spectrom 2001, 12, 716–725) © 2001 American Society for Mass Spectrometry

The development of the soft ionization techniques of electrospray ionization (ESI) [1] and matrix-assisted laser desorption ionization (MALDI) [2] has extended the field of mass spectrometry to the study of the structure and conformation of gas-phase biomolecules. In addition to being routinely used to obtain the molecular weight of intact protein and oligonucleotide ions, electrospray ionization mass spectrometry is also widely used for the investigation of non-covalent interactions present in solution, such as those between protein-ligand pairs [3], protein-DNA complexes [4], and double-stranded oligonucleotide ions [5], among many others. In addition, it has been demonstrated that electrospray ionization can be used to produce extensively solvated gas-phase biomolecules [6], opening the door for the study of the protein solvation process one water molecule at a time. However, the relationship between the chemistry of an analyte in solution and its gas-phase behavior, as reflected by its abundance in the electrospray-generated mass spectra and its gas-phase reactivity, has not been completely elucidated.

Previous studies have provided evidence indicating that noncovalent interactions present in solution can in fact be preserved through the electrospray process, and that the mass spectral ion intensities are a reflection of the abundance of such ions in solution. For example, Henion and coworkers [7] used ion spray mass spectral ion intensities to determine the equilibrium dissociation constants (K_D) for complexes between some vancomycin group antibiotics and cell-wall peptide ligands. Good agreement with solution K_D values was reported, indicating that the affinity observed in solution is preserved in the gas-phase complexes. Electrospray mass spectral studies by Chait and coworkers [8] of aqueous cytochrome *c* solutions showed significant differences in the protein charge state distributions as a function of pH, suggesting a direct correlation between solution and gas-phase conformations. However, there is also experimental evidence supporting the lack of a direct relationship between the ions present in the gas phase and the initial solution conditions. Wang and Cole [9] used the small peptides gramicidin S and bradykinin as test compounds in order to examine the effect of solution pH in their electrospray charge state distributions. The authors observed that significant pH changes in solution only lead to relatively minor changes in the distribution of singly and doubly pro-

Published online May 2, 2001

Address reprint requests to Dr. Joel H. Parks, The Rowland Institute for Science, 100 Edwin H. Land Boulevard, Cambridge, MA 02142, USA.
E-mail: parks@rowland.org

tonated gas-phase ions for these peptides. Discrepancies between solution equilibria and gas-phase charge state distributions indicated the electrospray ionization (ESI) mass spectrum obtained is far from reflecting solution-phase conditions. Clearly, studying the nature and origin of these similarities and discrepancies is desirable in order to obtain a better understanding of the electrospray process and its effect on the properties of solution analytes.

Spectroscopic measurements can help to investigate the conformation and structural changes that biomolecules undergo during their transfer from solution to the gas phase via electrospray ionization. At the same time, such studies may also bring a better understanding of the ESI process itself and its effect on solution species. Konermann and Douglas [10] studied the acid-induced denaturation of cytochrome *c* using circular dichroism, absorption, and fluorescence solution measurements in combination with electrospray ionization experiments in order to investigate the relationship between the solution protein conformation and charge state distributions observed in the ESI mass spectra. The authors concluded that the charge state distribution generated during ESI was not sensitive to changes in the secondary structure, but related to the breakdown of the protein tertiary structure. Recently, Van Berkel and co-workers [11] measured the fluorescence excitation spectra of the analyte octaethylporphyrin in the electrospray stream. The authors found good correlation between the excitation fluorescence spectra and absorption measurements in solution, but not with the ions detected in the mass spectrum. The mass spectral discrepancies were attributed to gas-phase reactions occurring late in the electrospray process. More recently, Cook and coworkers [12] determined the pH of electrospray droplets by monitoring the fluorescence of a pH-sensitive chromophore within the spray stream. Results demonstrate that for unbuffered solutions, both positive and negative electrospray operating modes result in slight but noticeable spectral changes, indicating pH changes within the spray droplets, $\Delta\text{pH} \leq 1$.

Efforts in our laboratory [13] have recently been directed toward using fluorescence spectroscopy measurements to investigate the effects that the electrospray process may have on the structure and conformation of peptides and proteins. In this work, the fluorescence of the protein horse heart cytochrome *c* during electrospray is investigated and compared with analogous fluorescence measurements in solution. Horse heart cytochrome *c* is a 104-amino acid protein containing a single tryptophan residue on position 59 and a heme group that is covalently linked to cysteine residues on position 14 and 17 [14]. In its native conformation, the indole side chain of Trp-59 is hydrogen bonded to one of the propionate groups of the heme. The proximity of these two residues results in the quenching of the tryptophan fluorescence via resonance energy transfer to the heme. However, as the protein unfolds, the effective distance between Trp-59 and the heme group

increases and a subsequent increase in the fluorescence of Trp results. This characteristic has made of cytochrome *c* a commonly used probe for protein folding studies using fluorescence emission spectroscopy [15]. By varying the amount of alcohol in the electrosprayed solutions, protein denaturation is induced and the resulting conformational changes are studied by monitoring the fluorescence intensity of Trp-59. It is not our purpose to measure specific denaturation parameters, but to use the protein intrinsic fluorescence as a probe for differences between the electrospray and bulk-solution environments under similar denaturation conditions. This understanding will be essential for the interpretation of future fluorescence measurements of trapped protein ions generated by electrospray ionization.

Experimental

Fluorescence Spectroscopy

A schematic of the experimental setup is shown in Figure 1. Fluorescence experiments are performed using radiation at 266 nm obtained from the fourth harmonic of a Nd:YAG laser. This light source produces pulses of 20 nanoseconds duration at a repetition rate of 10 Hz. Following a series of optical elements which set the laser intensity and beam diameter, the UV light beam is split into two beams, A and B, to be used for the electrospray and solution experiments, respectively. The experimental setup is designed so that both electrospray and solution fluorescence emission experiments could be performed using the same detection assembly. The incident laser light is directed into the analysis box C (see Figure 1) in which either the electrospray mounting or the solution cuvette is located. The laser alignment and focusing conditions resulted in an excitation laser beam diameter of ~ 1 mm for solution experiments and of ~ 2 mm for electrospray. The fluorescence emitted is collected at a 90° angle from the incident light, and focused into the entrance slit of a 0.5 m spectrometer (SpectraPro 500, Acton Research Corporation, Acton, MA). All the spectra presented in this work were acquired using a 1200 grooves/mm grating (blaze wavelength = 300 nm) at a scanning rate of 50 nm/minute over the range of 275–525 nm. The fluorescence is detected at the spectrometer exit by a photomultiplier tube (PMT) (Model R1463, Hamamatsu, Toyooka Vill., Japan). For bulk-solution fluorescence experiments, the entrance and exit slits of the spectrometer were opened to 0.5 mm and the PMT voltage was -700 V. For electrospray fluorescence experiments, the slits were opened to 1.5 mm with the PMT operating at -1000 V. These detection parameters provided a resolution of 0.8 and 2.5 nm for bulk-solution and electrospray measurements, respectively. The output signal, which was simultaneously monitored by an oscilloscope (Model 7104, Tektronix, Pittsfield, MA), was amplified and then analyzed by a

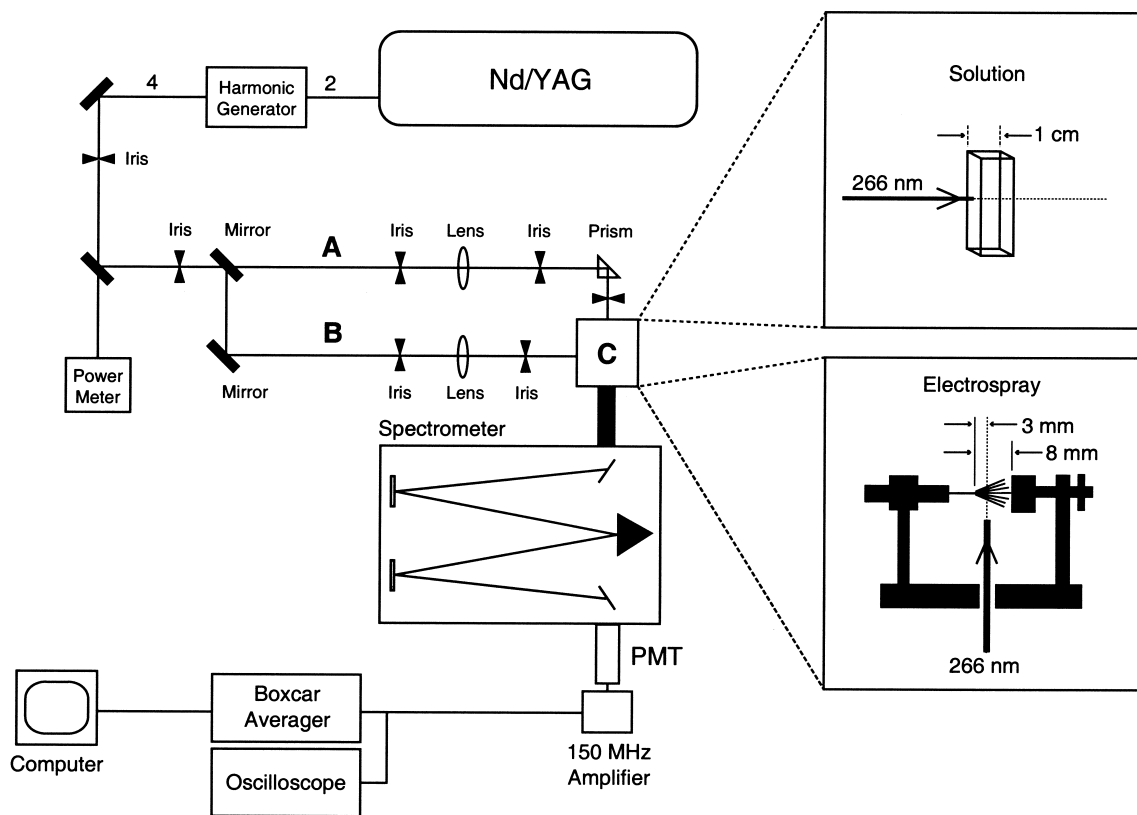


Figure 1. Schematic of the instrumental set up used for measurements of the solution and electro spray fluorescence emission spectra. A and B represent laser beams used for electro spray and bulk-solution measurements, respectively. C represents position of sample box containing the electro spray plume and cuvette setups.

boxcar integrator (Stanford Research Systems, Model 5580). In order to take into account pulse-to-pulse laser fluctuations, the fluorescence output signal was divided by a signal obtained from the incident laser pulse and the resulting fluorescence spectra collected and stored using LabView software (National Instruments, Austin, TX). Final spectra collected are plots of boxcar integrator output (last 30 samples averaged) as a function of wavelength.

The analyte fluorescence can be monitored either by measuring it at a specific wavelength (340 nm) or by integrating the collected spectrum over the 285–450 nm window, obtaining a value for the total fluorescence emitted. Unless otherwise noted, fluorescence values reported in this work were obtained using the latter integration method. Further data analysis included subtraction of background fluorescence and correction for the combined spectrometer and detector wavelength response.

Sample Preparation

Horse heart cytochrome *c* was obtained from Sigma Chemical Co. (St. Louis, MO) and used without further purification. Stock solutions of the protein were prepared using deionized water. For alcohol denaturation

experiments, aliquots of the stock solutions were diluted with spectral-grade methanol (Fisher, Pittsburgh, PA) or 1-propanol (Fisher) to obtain solutions with different alcohol content. Analyte concentrations were not determined spectrophotometrically. The pH of the solutions was adjusted to pH = 4 using acetic acid (Fisher). All pH measurements were performed using a PerpHecT LogR pH meter (Orion Research, Inc., Beverly, MA) and a semi-micro combination pH electrode (Orion Research, Inc.). Reported pH values are not corrected for methanol.

Electrospray Measurements

Solutions were delivered to the electro spray needle, or emitter, through a fused silica capillary line (100 μm i.d.) at a flow rate of 2 $\mu\text{L}/\text{min}$ using a syringe pump (Harvard Apparatus, Holliston, MA). A stainless steel zero-dead-volume capillary mini-union (Scientific Instrument Services, Ringoes, NJ) provided electrical contact between the solution and the Al-clad fused silica capillary tubing (Scientific Instrument Services) employed as the electro spray needle (100 μm i.d.). The electric field necessary for electro spray was obtained by applying a high voltage (2.2–3.8 kV) to the capillary mini-union. The ESI plume of positively charged drop-

lets is aligned horizontally between the needle and the 1 cm diameter stainless steel counter-electrode, positioned 8 mm downstream and kept at ground potential (Figure 1, lower inset). The electrospray needle and counter-electrode are mounted on a common platform that can be adjusted relative to the laser beam using a miniature xy translation stage (Newport Corporation, Irvine, CA). The electrospray is intersected vertically (parallel to the spectrometer slits) by the laser light with the center of the laser beam positioned 3 mm from the needle tip. Overlap of the electrospray plume and the laser beam diameter results in a sampling volume of approximately 12 mm^3 . Background fluorescence spectra were acquired by electrospraying the solvent solutions (without the fluorescent analyte) under similar operating conditions.

Solution Measurements

A 10 mm path length quartz cuvette (Wilma Glass Company, Inc., Buena, NJ) was used to measure both the bulk-solution fluorescence spectra of the analytes and the corresponding solvent background fluorescence. The incident 266 nm laser beam enters the analysis box C (Figure 1) through a side panel aperture and intersects the solution sample horizontally (perpendicular to spectrometer slits). The fluorescence emitted is collected at a 90° angle using the same spectrometer/detection assembly as in the electrospray experiments.

Results and Discussion

Fluorescence Dependence on Analyte Concentration and Laser Intensity

The dependence of the bulk-solution and electrospray fluorescence on both analyte concentration and incident laser power was investigated in order to determine the appropriate experimental conditions to avoid aggregation and/or photodegradation effects during the denaturation experiments. For the concentration dependence experiments, solutions of cytochrome *c* (20:80 H₂O/MeOH; pH = 4) were prepared at various concentrations and the electrospray and solution fluorescence spectra were measured. High MeOH solutions were used to insure mostly unfolded and fluorescent proteins were probed. The range of concentrations investigated varied between 10^{-6} and 10^{-4} M for electrospray measurements and between 10^{-7} and 10^{-5} M for bulk measurements. Figure 2 a, b show graphs of fluorescence as a function of cytochrome *c* concentration obtained from solution and electrospray measurements, respectively. Fluorescence values and error bars reported were obtained by monitoring the protein emission at 340 nm during 1 minute. For each solution, a total of 600 single-shot measurements were collected at the indicated wavelength, and the corresponding error bars represent one standard deviation from the average values. Concentration dependence experiments in solu-

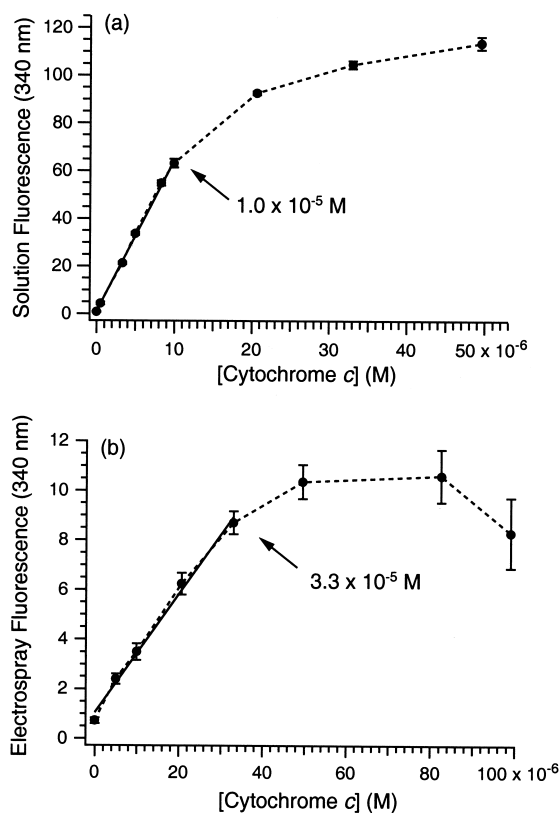


Figure 2. Dependence of cytochrome *c* fluorescence (monitored at 340 nm) on concentration for (a) bulk solution and (b) electrospray experiments. Data obtained using 20:80 H₂O/MeOH solutions of the protein at pH = 4. Laser powers used were 16 kW/cm² and 1.2 MW/cm² for solution and electrospray experiments, respectively.

tion indicate a linear response region extending up to about 1.0×10^{-5} M for cytochrome *c*. For the electrospray experiments, linearity was observed up to a cytochrome *c* concentration of about 3.3×10^{-5} M. At higher protein concentrations, deviation from linearity and a decrease in fluorescence was observed, consistent with the expected aggregation and/or inner-filter effects [16]. Therefore, to have sufficient signal-to-noise ratio (S/N) but to avoid any concentration effects, protein concentrations of 3×10^{-5} and 3×10^{-6} M were used for the electrospray and solution denaturation experiments, respectively.

The dependence of solution and electrospray fluorescence on incident laser power was also investigated in order to determine the appropriate conditions to avoid photodegradation of the samples and detector saturation. Two cytochrome *c* solutions were prepared using a 20:80 H₂O/MeOH solvent ratio, in order to obtain mostly denatured and fluorescent proteins, and their pH was adjusted to 4. For solution and spray measurements, the protein concentration was approximately 5×10^{-6} and 5×10^{-5} M, respectively. For the spray measurements, the use of a cytochrome *c* concentration slightly higher than the upper limit obtained from concentration dependence experiments is not ex-

pected to affect the results significantly. Under the instrumental conditions used, the peak laser intensity was varied between 16 and 100 kW/cm² for solution experiments, and between 0.3 and 1.6 MW/cm² for electrospray measurements. The cytochrome *c* fluorescence response was found to be linear over the entire range of laser intensities for both solution and spray experiments, indicating the absence of photodegradation or saturation effects for this protein. Final fluorescence experiments were performed using incident peak laser intensities of 20 kW/cm² (3 μJ/pulse) and 0.9 MW/cm² (0.6 mJ/pulse) for solution and electrospray denaturation measurements, respectively.

Alcohol Denaturation of Cytochrome *c*

Changes in the cytochrome *c* conformation were induced by using increasing amounts of alcohol as co-solvent, and monitored by measuring the total emitted fluorescence. The addition of an organic co-solvent, like methanol, to a native-protein solution results in the unfolding or denaturation of the protein [15d,e]. Figure 3 shows the (a) electrospray and (b) bulk-solution fluorescence emission spectra obtained for cytochrome *c* in different H₂O/MeOH solutions. At low alcohol content, protein fluorescence is not detected, indicating that cytochrome *c* molecules within the droplets as well as in solution are in a compact or folded conformation. At high methanol content, a significant increase in the protein fluorescence is detected and the characteristic fluorescence spectra are observed.

By measuring the extent of protein fluorescence at a constant position within the electrospray plume for solutions of different solvent composition, the denaturation process can be followed. Figure 4 shows plots of total cytochrome *c* fluorescence as a function of methanol obtained from measurements in bulk solution (open circles, solid line) and within the electrospray plume (filled circles, dashed line). The error bars reported represent 2 times the standard deviation values, which were calculated from multiple total fluorescence measurements using each protein solution. The electrospray data have been scaled by multiplying by a factor of 5 (filled circles, solid line) in order to allow an appropriate comparison with the solution denaturation curve. The choice of a multiplying factor is arbitrary and it is only meant to approximate normalization. Error bars have been scaled appropriately. For droplet measurements, no fluorescence is detected for solutions containing 45% MeOH or less, indicating the proteins must be in a folded conformation within the electrospray droplets. As the fraction of MeOH is increased, a slow but steady increase in the protein fluorescence is detected, reaching a maximum fluorescence at 90% MeOH. Solutions of higher methanol content were avoided due to protein insolubility. The increase in electrospray protein fluorescence at high MeOH content is consistent with the presence of unfolded or partially denatured proteins within the electrospray droplets.

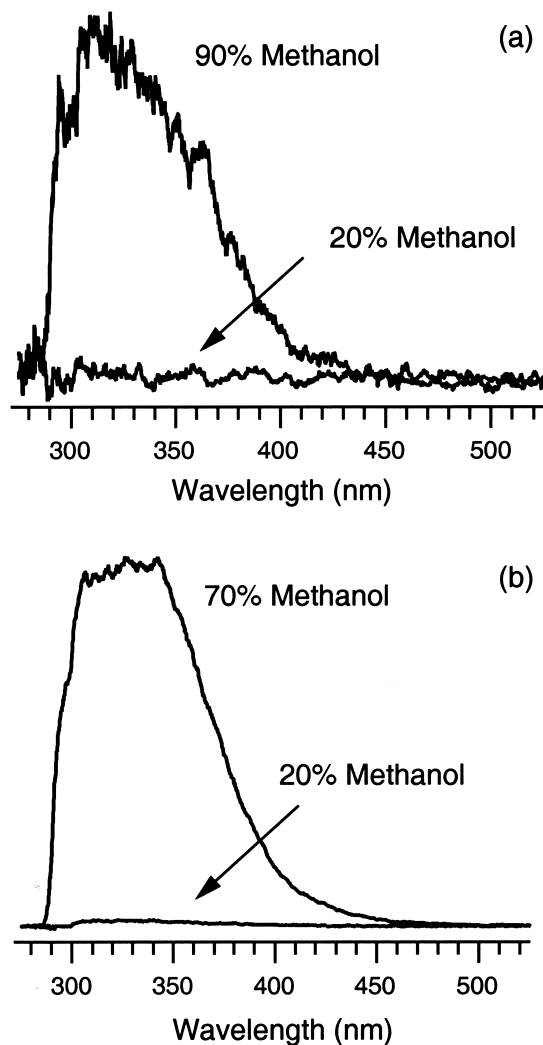


Figure 3. Fluorescence emission spectra obtained from (a) electrospray and (b) solution measurements of cytochrome *c* samples at high and low percentages of methanol. The protein concentration is $\sim 3 \times 10^{-5}$ M for electrospray measurements and $\sim 3 \times 10^{-6}$ M for solution. The pH was adjusted to 4.

Comparison of electrospray and solution experiments reveals one distinctive feature: the cytochrome *c* denaturation curve obtained from bulk solution differs from that obtained from droplet measurements. This difference was reproduced in repeated experiments comparing solution and droplet fluorescence. For bulk-solution measurements, no fluorescence is detected at low methanol content ($\leq 40\%$ MeOH) indicating, as for droplet experiments, folded protein conformations. The onset of fluorescence, which indicates the initiation of the unfolding process, occurs around 40% MeOH for solution. At higher alcohol content, however, differences between droplet and solution measurements are significant. The solution results show a sharp increase in fluorescence intensity between 40 and 60% methanol, after which the protein fluorescence plateaus. Such a sharp increase is not observed during the droplet measurements. On the contrary, the increase in fluorescence

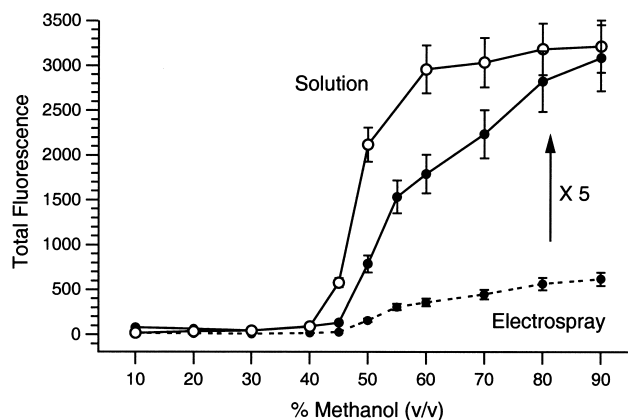


Figure 4. Plots of total cytochrome *c* fluorescence (285–450 nm) as a function of methanol concentration obtained from solution (open circles, solid line) and electrospay (filled circles, dashed line) experiments. The electrospay data have been scaled by a factor of 5 (filled circles, solid line) for comparison.

intensity with methanol during electrospay measurements appears to be reduced, with the highest fluorescence intensity recorded at 90% methanol. Differences in the relative extent of fluorescence for similar H₂O/MeOH ratios suggest different droplet and solution protein conformations. Moreover, fluorescence measurements appear to indicate proteins within the droplets have refolded to more compact conformations than those present in solutions of similar composition. Such a change in conformation could be the result of protein exposure to different environments in the droplet and in solution. Here we consider two factors that could affect the extent of protein fluorescence within electrospay droplets: solvent evaporation and droplet surface effects.

Solvent Evaporation. The effect of evaporation on a heterogeneous droplet (composed of more than one solvent) is expected to result in the faster evaporation of that solvent with the higher vapor pressure and an enrichment in the less volatile one. Zhou and Cook have recently investigated the extent of solvent evaporation and fractionation within spray droplets [17]. Their experiments on acetone/water, acetonitrile/water, and acetone/ethylene glycol droplets indicate a gradual enrichment of the less volatile solvent along both the axial and lateral profiles of the spray. For the H₂O/MeOH solutions used in our experiments, methanol is the component with the higher vapor pressure [at 25 °C: $P_{\text{vapor}}(\text{MeOH}) = 126.8$ Torr and $P_{\text{vapor}}(\text{H}_2\text{O}) = 23.8$ Torr] [18]. This would result in a lower methanol fraction in the droplets than in the original solutions. This could explain the need for even higher methanol content (lower H₂O) within the droplets in order to observe a similar extent of unfolding as in solution. In order to further investigate and evaluate the role of solvent evaporation in droplet fluorescence measurements, the denaturation of cytochrome *c* by propyl

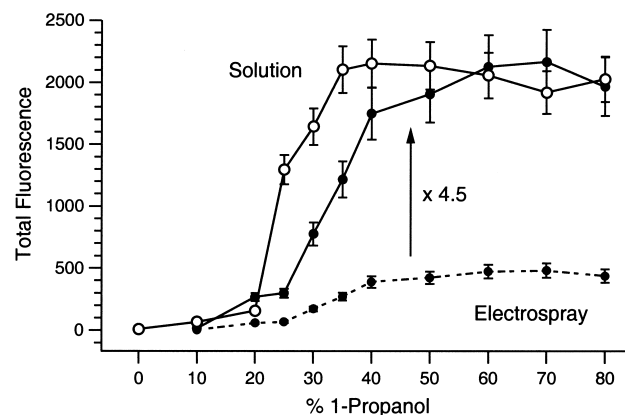


Figure 5. Plots of total cytochrome *c* fluorescence (285–450 nm) as a function of 1-propanol concentration obtained from solution (open circles, solid line) and electrospay (filled circles, dashed line) experiments. The electrospay data have been scaled by a factor of 4.5 (filled circles, solid line) for comparison.

alcohol (1-propanol or 1-PrOH) was also investigated. This alcohol denaturant was selected because its vapor pressure is similar, in fact slightly lower [$P_{\text{vapor}}(1\text{-PrOH}) = 20.7$ Torr at 25 °C] [18], than that of water. Therefore, solvent evaporation would be significantly reduced for H₂O/1-PrOH than for H₂O/MeOH droplets. Figure 5 shows 1-PrOH denaturation curves obtained from cytochrome *c* fluorescence measurements in solution (open circles, solid line) and within the electrospay plume (filled circles, dashed line). Error bars represent two times the standard deviation values obtained from multiple total fluorescence measurements using each protein solution. Similar to the MeOH experiments, the electrospay data have been multiplied by a factor of 4.5 (filled circles, solid line) in order to illustrate a reasonable comparison with the solution denaturation curve. The solvent compositions investigated ranged from 0 to 80% 1-PrOH for solution experiments, and between 10 and 80% 1-PrOH for electrospay. Solutions containing more than 80% 1-PrOH were avoided due to protein insolubility. The onset of protein unfolding is observed around 20 and 25% 1-PrOH for solution and electrospay experiments, respectively. These are lower percentages than those needed to trigger methanol denaturation in cytochrome *c*, consistent with 1-PrOH being a better denaturant [19]. It is noted, however, that the electrospay denaturation curve is still displaced to higher percentages of 1-PrOH relative to solution, similar to results from electrospay methanol-denaturation experiments. For example, while a maximum in bulk-solution fluorescence intensity is already observed around 35% 1-PrOH, maximum fluorescence in droplets is only approached for solution containing 60 to 70% 1-PrOH. These results indicate that discrepancies between solution and electrospay denaturation curves as a function of alcohol content are not strongly correlated with solvent evaporation from the droplets.

In the following analysis, the extent of solvent evaporation from droplets of mixed composition is estimated. To determine the degree of evaporation that has occurred within the time window available for droplets to propagate to the sampling position (3 mm from the electrospray needle), it is necessary to estimate the droplet diameter and also the propagation time. The average primary droplet diameter [20,21] under our spray conditions is $\sim 3\text{--}4\ \mu\text{m}$ and decreases slightly ($\sim 12\%$) over the alcohol range of 20–80%. For the concentrations used ($\sim 3 \times 10^{-5}\ \text{M}$), these diameters yield charge densities greatly in excess of the Rayleigh limit. In this case, fission will occur immediately, resulting in the rapid formation of droplets having diameters of $<1\ \mu\text{m}$ which essentially contain all the charge. This conclusion follows from a calculation of asymmetric fission based on the measurements of Gomez and Tang [20a]. The following calculation estimates the time it takes for a $1\ \mu\text{m}$ diameter droplet to propagate along the axial z direction to the excitation position.

The droplet axial velocity is determined by the droplet mobility in air and the electrostatic field. A “far field” approximation ($z \gg r_c$) for the axial field, E_z , is derived from ref 20b as a function of the axial distance z ,

$$E_z = \frac{\Phi_o}{\ln\left(\frac{4z_o}{r_c}\right)} \frac{2z_o}{z(2z_o - z)} \quad (1)$$

where $\Phi_o = 3\ \text{kV}$ is the voltage applied across a distance of $z_o = 8\ \text{mm}$ between the needle tip and the ground counter-electrode, and $2r_c = 335\ \mu\text{m}$ is the outer diameter of the electrospray needle. The mobility of a $1\ \mu\text{m}$ diameter droplet in air is estimated from ref 22 to be $\mu_o \sim 1\ \text{cm}^2/\text{V}\cdot\text{s}$. The droplet charge was calculated for $\sim 3 \times 10^{-5}\ \text{M}$ solutions assuming an average charge state of $\langle z \rangle = 10$ for cytochrome c in a pH = 4 solution [10] and that most of the excess charge resides on the protein. Changes in average charge state might occur as a function of methanol concentration, but they are not considered in these estimates. The propagation time over a distance z_1 is given by the integral [21c]

$$t_{prop} = \int_0^{z_1} \frac{dz}{\mu_o E_z(z)} \quad (2)$$

which yields a propagation time of $t_{prop} = 60\ \mu\text{s}$ for a droplet to travel from the needle tip to the excitation laser position at $z_1 = 3\ \text{mm}$.

To consider the degree to which the MeOH fraction may vary, it was assumed that the MeOH was evaporating uniformly from the droplet surface area. The droplet mass loss rate and change in volume fraction were estimated as follows. The MeOH volume fraction, P_{MeOH} , can be expressed by

$$P_{\text{MeOH}} = \frac{V_m}{V} = \frac{V_{m_o} - \Delta V}{V_o - \Delta V} \quad (3)$$

where V_m is the MeOH volume, V is the droplet volume, V_o and V_{m_o} are the droplet and MeOH volume in the absence of evaporation, respectively. The change in droplet volume, ΔV , is essentially the change in methanol volume fraction, ΔV_m , since the water contribution $\Delta V_w \approx 0$ for $t_{prop} = 60\ \mu\text{s}$. The rate of volume change for a droplet of radius r is related to the mass loss rate due to evaporation by $\rho_m(dV/dt) = (dm/dt)_r$, where ρ_m is the methanol density and t_{prop} is defined above. Using the mass loss rate given in ref 21a for a droplet of initial volume $V_o = 4\pi r_o^3/3$, the change in droplet volume is given by

$$\Delta V = (V_o - V) = V_o \left\{ 1 - \left(1 - \frac{\beta t_{prop}}{r_o} \right)^3 \right\} \quad (4)$$

The coefficient β , determining the rate of change in droplet radius, is proportional to the methanol vapor pressure. For a pure methanol droplet, $\beta = \beta_o = 1.2 \times 10^{-3}\ \mu\text{m}/\mu\text{s}$ [21a]. The evaporation rate at the surface of a droplet, which is composed of a mixture of solvents, is determined by the rate solvent molecules can diffuse to the surface assuming that desorption is not rate limiting. Since the equilibrium methanol vapor pressure is a factor of ~ 5 greater than water, it is sufficient to consider that evaporation from the $\text{H}_2\text{O}/\text{MeOH}$ droplets results in loss of only the methanol fraction. In this case, the methanol vapor pressure is determined by an evaporation rate which is proportional to M_m/τ_D , where M_m is the methanol molarity and τ_D the characteristic time for methanol diffusion to the droplet surface, $\tau_D \propto 1/D$. The self diffusion of methanol within a $\text{H}_2\text{O}/\text{MeOH}$ droplet depends on a diffusion constant, D [23], approximated by

$$D \approx \frac{kT}{c(M_m\eta_m + M_w\eta_w)} \quad (5)$$

where M_m (M_w) is the molarity and η_m (η_w) is the viscosity of methanol (water) and c is a constant.

Defining the methanol vapor pressure for a heterogeneous droplet, p , in terms of the methanol vapor pressure for a pure methanol droplet, p_o , we have

$$p = p_o \left\{ \frac{M_m\eta_m}{M_m\eta_m + M_w\eta_w} \right\} \quad (6)$$

and

$$\beta = \beta_o \left\{ \frac{M_m\eta_m}{M_m\eta_m + M_w\eta_w} \right\} \quad (7)$$

This expression for β is used to calculate the change in droplet volume using eq 4 and finally the methanol

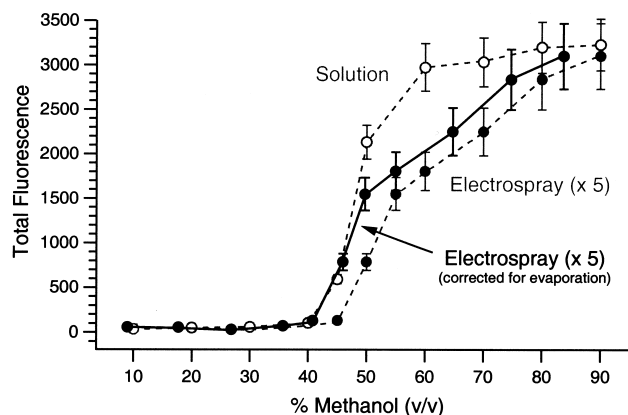


Figure 6. Cytochrome *c* droplet fluorescence curve obtained after correction for MeOH evaporation (filled circles, solid line). Also shown for comparison are the original bulk-solution and the scaled electro spray data (dashed lines).

volume fraction using eq 3 for a droplet of initial radius $r_o = 0.5 \mu\text{m}$ and $t_{\text{prop}} = 60 \mu\text{s}$. The cytochrome *c* fluorescence data obtained from droplet experiments can be corrected and the methanol fraction can be scaled in order to reflect droplet rather than solution composition. The result of this re-scaling is shown in Figure 6. As observed, the discrepancy between the spray and solution measurements is not resolved by this re-scaling.

It must be noted that changes in the MeOH fraction might give rise to variations in chromophore number density within the laser excitation volume. We are unable to quantitatively determine the extent and/or effect of such possible variations. Therefore, it is assumed that the electro spray denaturation curves observed are predominantly the result of protein conformational changes as a function of solvent composition.

Droplet Surface Effects. The droplet/air interface of an electro spray droplet could provide a significantly different environment in which the protein could refold adequately to affect the extent of protein fluorescence. In this section we estimate the extent of protein diffusion to the droplet surface and suggest how protein adsorption at this interface could lead to changes in the fluorescence emission. In these measurements of protein fluorescence spectra, achieving an adequate signal-to-noise ratio (S/N) required a droplet charge density a factor of $\sim 10^3$ greater than densities previously used to investigate the dynamics of droplet fission [20,21]. The following analysis, like the previous estimates, relies on extrapolating the understanding developed for lower charge densities to estimate processes occurring at densities used in these experiments.

Cytochrome *c* ions will diffuse to the surface from a distance r_{diff} given by [24]

$$r_{\text{diff}}^2 \approx \pi D t_{\text{prop}} \quad (8)$$

where D is the protein diffusion coefficient. Due to the lower viscosity of MeOH, eq 5 implies the diffusion coefficient of cytochrome *c* in $\text{H}_2\text{O}/\text{MeOH}$ droplets increases by a factor of ~ 2 as the fraction of MeOH varies from 10–80%. In pure water droplets, $D_{\text{cyt},c} \approx 10^{-6} \text{ cm}^2/\text{s}$ [25], resulting in a range of $r_{\text{diff}} \approx 0.14$ to $0.2 \mu\text{m}$. This range of r_{diff} indicates that, depending on the methanol fraction, approximately 65–80% of the protein molecules in a $1 \mu\text{m}$ diameter droplet can diffuse to the droplet/air interface during a propagation time of $t_{\text{prop}} \sim 60 \mu\text{s}$ before exposure to the 266 nm excitation beam. It should be mentioned that diffusion coefficients derived from measurements of diffusion limited adsorption of proteins near an air/water interface have been observed to be significantly greater than values estimated by the Einstein equation [26]. It was suggested that convection was probably contributing to particle motion near such an interface.

The diffusion and adsorption of proteins to non-polar surfaces have been previously investigated. Gast and coworkers [27] have measured the adsorption rate of native-state ribonuclease A at the non-polar interface of polystyrene spheres in $\text{H}_2\text{O}/\text{MeOH}$ solutions. The hydrophobic interaction between the protein and the spheres was considered to be a major driving force for adsorption. Proteins adsorbed at the non-polar surface of the spheres were in a more hydrophobic environment in which the free energy was minimized by reducing the amount of structured water at the protein surface. The observed adsorption rate is highest for pure water and decreases as the methanol fraction increases, suggesting that methanol itself reduces the tendency of water structuring at the interface so that adsorption does not provide as much free energy advantage. In our experiments, the droplet surface could serve as the hydrophobic interface to provide a similar driving force for cytochrome *c* adsorption.

The adsorption of bovine serum albumin (BSA) [28] and lysozyme [29] at the air/water interface has been studied by neutron reflection. These studies show evidence indicating that at densities ($\sim 10^{-4} \text{ g}/\text{cm}^3$) comparable to those in our experiments, proteins can form monolayers and can protrude above the water surface. Although BSA becomes slightly distorted in the surface environment, neither lysozyme nor BSA show evidence indicating their globular framework is denatured.

These previous studies provide evidence supporting the diffusion and adsorption of cytochrome *c* molecules at the droplet/air interface. The following equation for the total fluorescence power, P_{ESI} , emitted by electro spray droplets is useful to describe the experimental differences observed between bulk-solution and electro spray denaturation curves in the presence of diffusion and adsorption at the droplet/air interface.

$$P_{\text{ESI}} = N_B p_B + N_S p_S \quad (9)$$

Here, N_S is the number of proteins adsorbed at the droplet surface and N_B is the number of proteins remaining in the bulk of the droplet. For 1 μm diameter droplets, $N = (N_S + N_B) \approx 10^4$ proteins for the molarities used. Note that the diffusion dependence on viscosity shown in eq 5 implies that N_S will vary with alcohol fraction. The fluorescence power radiated by a surface (bulk) protein is p_S (p_B) and both of these fluorescence rates will depend on the alcohol fraction, on the environment surrounding the fluorescent molecule, and therefore, on the protein conformation. If we assume that p_B has identical characteristics to solution fluorescence, then our denaturation data suggest that $p_S \leq p_B$ so that the total fluorescence power from N proteins in droplets could be less than N proteins in bulk solution. The following discussion considers the alcohol dependence of the denaturing curves in terms of the variations in both N_S and p_S .

As presented in our estimates of cytochrome *c* diffusion, more than 80% of the proteins contained in a ~ 1 μm diameter droplet are expected to diffuse to its surface at high ($>80\%$) MeOH concentrations. Under these conditions, denatured proteins are expected to dominate and give rise to the maximum in fluorescence detected. That is, P_{ESI} would be approximated by Np_S . At low methanol concentrations ($<40\%$), the high water content and lower cytochrome *c* diffusion would lead to a lower droplet-surface population, resulting in a droplet environment similar to that of bulk solution, and consequently a fluorescence response ($P_{\text{ESI}} \sim Np_B$) consistent with the presence of compact, folded structures, for which $p_B \sim 0$, in both spray and bulk-solution measurements. At intermediate $\text{H}_2\text{O}/\text{MeOH}$ ratios, the fluorescence response of proteins at the surface has been observed to be reduced from that in bulk solution, $p_S < p_B$. This response could result from a higher molecular/charge density at the surface due to the intermediate protein diffusion coefficients, as well as from the effects of the changing dielectric environment. It is possible that as the solvent environment varies from a high to a low water concentration to a lower dielectric medium (air/droplet interface), proteins are actively competing for solvation by water or alcohol and intramolecular charge solvation. This could result in refolding to achieve more compact structures than those expected in bulk-solution where surface effects are absent. The possibility of refolding partially denatured cytochrome *c* molecules within a time interval of $t_{\text{prop}} \sim 60$ μs is supported by studies discussed and cited in ref 30.

The discussion above describes the role of adsorption in the fluorescence behavior of cytochrome *c* molecules within electrospray droplets. There are additional phenomena which may be contributing to variations of the protein dynamics at the droplet surface. For example, an excess MeOH fraction [31] is expected near the droplet/air interface resulting from the different surface tensions of MeOH and water (0.22 and 0.76 mN/cm, respectively) [18]. However, such an

excess may be compensated by preferential loss of MeOH resulting from the greater evaporation rate relative to water. At the very least, these processes introduce an uncertainty in the local MeOH fraction the adsorbed protein is exposed to within the surface environment. As previously mentioned, a simple re-scaling of the MeOH fraction will not bring the droplet and solution data shown in Figure 4 into closer agreement. The 1-PrOH droplet fluorescence data displays a similar deviation from the solution data and in this case evaporation corrections to the 1-PrOH fraction are negligible.

The study of radiative interactions of polarized radiation with molecules in droplets [32] considers several processes which can lead to changes in molecular fluorescence intensity when the molecules are at the droplet surface. Spherical droplet resonance effects are probably averaged out by the droplet size distribution in our experiments and are therefore not observed in our spray-fluorescence spectra (Figure 3a). However, this does not eliminate the possibility that these droplet resonances are contributing to the fluorescence variations observed in our experiments. Such effects could be evaluated by performing experiments with a single, well defined droplet size. Our measurements indicate that the denaturation curves obtained from droplet experiments are consistent with the presence of more compact or folded protein conformations than those described by the bulk-solution curves. It is our suggestion that changes in the protein structure are the result of diffusion and probable adsorption at the droplet/air interface during the time prior to laser excitation. However, the electrospray process is not understood adequately to rule out the possibility that droplet formation processes are contributing to the observed changes in protein conformation.

Conclusions

Protein fluorescence measurements within the electrospray plume and in bulk solution have been performed in an effort to obtain some information about the relative conformational differences between the solution and droplet environments. For solutions of intermediate methanol composition, comparison between electrospray and solution experiments suggests a lower extent of cytochrome *c* denaturation, or refolding, is observed within the droplets, indicating the conformation of electrosprayed proteins differs from that found in solutions of similar composition. Protein denaturation experiments using the low vapor pressure solvent 1-propanol indicate that differences between the droplet and solution measurements are not due to solvent evaporation effects. It is suggested that different droplet conformations are probably the result of exposure of the protein to a solvent environment that differs significantly from that of bulk solution. This would be the situation expected for a protein undergoing diffusion and adsorption to the droplet/air interface.

We have demonstrated that the combination of fluorescence spectroscopy and electrospray ionization provides insights into the effects the electrospray process has on solution analytes. Fluorescence studies on trapped ions would significantly increase our knowledge about the structure and conformation of gas-phase biomolecules. Current efforts in our laboratory are being directed toward this goal.

Acknowledgments

This work is financially supported by The Rowland Institute for Science. The authors acknowledge helpful discussions with Dr. John Osterhout, Dr. Jeff Hoch, and Dr. J. Foley, and thank Dr. S. Krückeberg for helping with the spectra acquisition software.

References

- (a) Fenn, J. B.; Mann, M.; Meng, C. K.; Wong, S. F.; Whitehouse, C. M. *Science* **1989**, *246*, 64–71. (b) Kebarle, P.; Tang, L. *Anal. Chem.* **1993**, *65*, 972A–986A. (c) Fenn, J. B.; Mann, M.; Meng, C. K.; Wong, S. F.; Whitehouse, C. M. *Mass Spectrom. Rev.* **1990**, *9*, 37–70.
- (a) Karas, M.; Hillenkamp, F. *Anal. Chem.* **1988**, *60*, 2299–2301. (b) Karas, M.; Bachmann, D.; Bahr, U.; Hillenkamp, F. *Int. J. Mass Spectrom. Ion Proc.* **1987**, *78*, 53–68.
- (a) Ogorzalek Loo, R. R.; Goodlett, D. R.; Smith, R. D.; Loo, J. A. *J. Am. Chem. Soc.* **1993**, *115*, 4391–4392. (b) Anderegg, R. J.; Wagner, D. S. *J. Am. Chem. Soc.* **1995**, *117*, 1374–1377.
- Cheng, X.; Hofstadler, S. A.; Bruce, J. E.; Harms, A. C.; Chen, R.; Terwilliger, T. C.; Goundreau, P. N.; Smith, R. D. In *Techniques in Protein Chemistry VII*; Marshak, D. R., Ed.; Academic Press: San Diego, CA, 1996; pp13–22.
- (a) Bayer, E.; Bauer, T.; Schmeer, K.; Bleicher, K.; Maier, M.; Gaus, H.-J. *Anal. Chem.* **1994**, *66*, 3858–3863. (b) Light-Wahl, K. J.; Springer, D. L.; Winger, B. E.; Edmonds, C. G.; Camp, D. G., II; Thrall, B. D.; Smith, R. D. *J. Am. Chem. Soc.* **1993**, *115*, 803–804.
- (a) Chowdhury, S. K.; Katta, V.; Chait, B. T. *Rapid Commun. Mass Spectrom.* **1990**, *4*, 81–87. (b) Smith, R. D.; Light-Wahl, K. J. *Biol. Mass Spectrom.* **1993**, *22*, 493–501. (c) Rodriguez-Cruz, S. E.; Klassen, J. S.; Williams, E. R. *J. Am. Soc. Mass Spectrom.* **1997**, *8*, 565–568. (d) Lee, S.-W.; Freivogel, P.; Schindler, T.; Beauchamp, J. L. *J. Am. Chem. Soc.* **1998**, *120*, 11758–11765.
- Lim, H.-K.; Hsieh, Y. L.; Ganem, B.; Henion, J. *J. Mass Spectrom.* **1995**, *30*, 708–714.
- Chowdhury, S. K.; Katta, V.; Chait, B. T. *J. Am. Chem. Soc.* **1990**, *112*, 9012–9013.
- Wang, G.; Cole, R. B. *Org. Mass Spectrom.* **1994**, *29*, 419–427.
- Konermann, L.; Douglas, D. J. *Biochemistry* **1997**, *36*, 12296–12302.
- Chillier, X. Fr. D.; Monnier, A.; Bill, H.; Gulacar, F. O.; Buchs, A.; McLuckey, S. A.; Van Berkel, G. J. *Rapid Commun. Mass Spectrom.* **1996**, *10*, 299–304.
- Zhou, S.; Edwards, A. G.; Cook, K. D.; Van Berkel, G. J. *Anal. Chem.* **1999**, *71*, 769–776.
- Parks, J. H.; Rodriguez-Cruz, S. E.; Khoury, J. T. *The 48th ASMS Conference on Mass Spectrometry and Allied Topics*; Long Beach, CA, 2000.
- Dickerson, R. E.; Takano, T.; Eisenberg, D.; Kallai, O.; Samson, L.; Cooper, A.; Margoliash, E. *J. Biol. Chem.* **1971**, *246*, 1511–1535.
- See for example: (a) Myer, Y. P.; MacDonald, L. H.; Verma, B. C.; Pande, A. *Biochemistry*, **1980**, *19*, 199–207. (b) Roder, H.; Elöve, G. A.; Englander, S. W. *Nature* **1988**, *335*, 700–704. (c) Elöve, G. A.; Chaffotte, A. F.; Roder, H.; Goldberg, M. E. *Biochemistry*, **1992**, *31*, 6876–6883. (d) Kamatari, Y. O.; Konno, T.; Kataoka, M.; Akasaka, K. *J. Mol. Biol.* **1996**, *259*, 512–523. (e) Bychkova, V. E.; Dujsekina, A. E.; Klenin, S. I.; Tiktopulo, E. I.; Uversky, V. N.; Ptitsyn, O. B. *Biochemistry* **1996**, *35*, 6058–6063.
- Willard, H. H.; Merritt, L. L., Jr.; Dean, J. A.; Settle, F. A., Jr. *Instrumental Methods of Analysis*; Seventh Ed.; Wadsworth Publishing Company: Belmont, CA, 1988; Chapter VIII.
- Zhou, S.; Cook, K. D. *Anal. Chem.* **2000**, *72*, 963–969.
- Lide, D. R. *CRC Handbook of Chemistry and Physics*; CRC Press: Boca Raton, FL, 1998–1999.
- Kaminsky, L. S.; Miller, V. J.; Davison, A. J. *Biochemistry* **1973**, *12*, 2215–2221.
- (a) Gomez, A.; Tang, K. *Phys. Fluids* **1994**, *6*, 404–414. (b) Tang, K.; Gomez, A. *Phys. Fluids* **1994**, *6*, 2317–2332.
- (a) Tang, L.; Kebarle, P. *Anal. Chem.* **1993**, *65*, 3654–3668. (b) Ikonomou, M. G.; Blades, A. T.; Kebarle, P. *Anal. Chem.* **1991**, *63*, 1989–1998. (c) Ikonomou, M. G.; Blades, A. T.; Kebarle, P. *Anal. Chem.* **1990**, *62*, 957–967. (d) Cole, R. B. *Electrospray Ionization Mass Spectrometry: Fundamentals, Instrumentation & Applications*; John Wiley & Sons: New York, NY, 1997; pp 15–25.
- Fuchs, N. A. *The Mechanics of Aerosols*; Pergamon Press Ltd.: Oxford, England, 1964; Chapter II.
- Bearman, R. J. *J. Phys. Chem.* **1961**, *65*, 1961–1968.
- McDaniel, E. W. *Collision Phenomena in Ionized Gases*; John Wiley & Sons: New York, NY, 1964; pp 502.
- Lehninger, A. L. *Biochemistry*; Worth Publishers, Inc.: New York, NY, 1979; pp 176.
- Song, K. B.; Damodaran, S. *Langmuir* **1991**, *7*, 2737–2742.
- Tilton, R. D.; Robertson, C. R.; Gast, A. P. *Langmuir* **1991**, *7*, 2710–2718.
- Lu, J. R.; Su, T. J.; Thomas, R. K. *J. Colloid Interface Sci.* **1999**, *213*, 426–437.
- Lu, J. R.; Su, T. J.; Howlin, B. J. *J. Phys. Chem.* **1999**, *103*, 5903–5909.
- Earon, W. A.; Muñoz, V.; Thompson, P. A.; Chan, C. C.; Hofrichter, J. *Curr. Opin. Struct. Biol.* **1997**, *7*, 10–14.
- Adamson, A. W.; Gast, A. P. *Physical Chemistry of Surfaces*; 6th Ed.; John Wiley & Sons: New York, NY, 1997; Chapter III.
- Folan, L. M.; Arnold, S. in *Topics in Fluorescence Spectroscopy: Biochemical Applications*; Vol. 3; Lakowicz, J. R., Ed.; Plenum Press: New York, 1992.